

# Laboratory Experiment and Application Evaluation of a Bio-Nano-depressurization and Injection-Increasing Composite System in Medium–Low Permeability Offshore Reservoirs

Qing Feng, Xianchao Chen,\* Ning Zhang, Xiaonan Li, Jingchao Zhou, Shengsheng Li, Xiaorong Zhang, Yanni Sun, and Yuehui She\*



Cite This: *ACS Omega* 2023, 8, 15553–15563



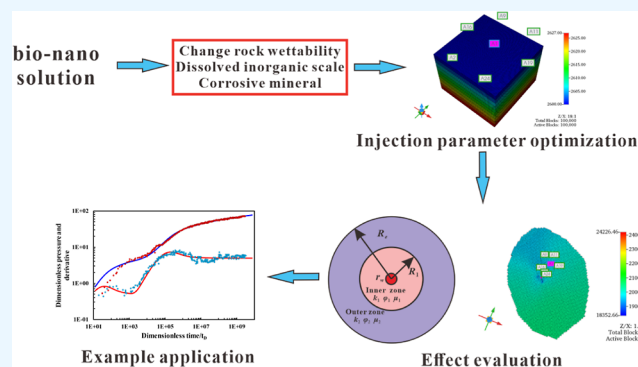
Read Online

ACCESS |

Metrics & More

Article Recommendations

**ABSTRACT:** Given the high injection pressure and insufficient injection volume in the offshore oilfield, Bohai Oilfield has developed a bio-nano-depressurization and injection-increasing composite system solution (bio-nano-injection-increasing solution) composed of bio-surfactants, hydrophobic nano-polysilicon particles, and dispersant additives. In response to the current problems, a new type of bio-nano-depressurization and injection enhancement technology has been studied, which has multiple functions such as nano-scale inhibition and wetting reversal. The new technology has the technical advantages of efficient decompression, long-term injection, and wide adaptation. However, there is still a lack of optimization schemes and application effect prediction methods, which hinder the further popularization and application of the bio-nano-composite system solution. To solve this problem, this paper takes Well A1 in the Bohai Sea as an example to optimize the injection volume, concentration, and speed of the bio-nano-augmentation fluid and evaluates the application effect by using the proposed well testing, water absorption index, and numerical simulation methods. The research results show that the bio-nano-injection fluid can effectively improve the reservoir permeability and reduce the injection pressure. The application effect evaluation method proposed is reliable and can provide some reference for similar depressurization and injection-increasing technologies.



## 1. INTRODUCTION

At present, due to poor reservoir physical properties and the hydration expansion of clay minerals, many offshore oilfields have a high water injection pressure, frequent operations, and an insufficient injection volume. At present, the mainstream solution is acidification and adding surfactants to reduce the pressure and increase the injection. However, after multiple rounds of acidification, the substances that can be dissolved in the reservoir are gradually reduced, and the validity period of the measures is gradually shortened or even invalid.<sup>1–3</sup> In addition, the application of conventional surfactants to offshore reservoirs still has some shortcomings, such as cost control, reduction of environmental damage, and applicability of high salinity seawater. To solve these problems, the Bohai Oilfield developed a new environment-friendly injection-increasing fluid—biological nano-depressurization and injection-increasing composite system (bio-nano-injection-increasing solution). The bio-nano-depressurization and injection-increasing composite system has the advantages of low cost and environmental friendliness when applied to offshore reservoirs, and its validity period exceeds that of conventional depressurization

and injection-increasing agents. The main components of the bio-nano-injection solution are hydrophobic nano-silica particles, bio-nano-surfactants, and dispersants. An appropriate amount of acid is added to form a composite system before field application to dissolve the inorganic scale plug and make the system easier to inject into the formation. After being injected into the water injection well, it drives away the pore hydration film around the bottom of the well to increase the pore seepage area and form a hydrophobic film of nano-thickness, resulting in water phase slip to reduce the seepage resistance,<sup>4–8</sup> thereby reducing the injection pressure of the water injection well. It has achieved very good results in the field pilot experiment in Bohai Oilfield.<sup>9–11</sup>

**Received:** February 10, 2023

**Accepted:** April 10, 2023

**Published:** April 18, 2023



**Table 1. Core Simulation Experiment Core Statistics**

number of cores	core size (length × diameter)	core source	permeability range (mD)	clay mineral content (%)	porosity range (%)
15	(2–2.5 cm) × 2.5 cm	artificial core	5–50	10–20	≈20
15	(3.5–4 cm) × 2.5 cm	artificial core	100–500	10–20	≈27

Scholars on the mechanism of nano-particle depressurization and injection enhancement have made a lot of elaborations and done experiments. After induction, there are mainly the following aspects: (1) Changing the wettability: the unsaturated bonds on the surface of nano-particles make them extremely hydrophobic. In the pores of the formation, the wettability of the rock surface will change due to intermolecular forces, hydrogen bonds, etc., so that the frictional resistance between the injected fluid and the formation pore throat will be greatly reduced, and the water phase permeability will increase. This point of view has also been demonstrated in related research and experiments. Ju et al.<sup>12</sup> described the drag reduction and injection enhancement mechanism of nano-particles as nano-scale or sub-nano-scale particles adsorbed on the porous surface of rocks, thus leading to changes in wettability, thereby increasing the relative permeability of the water phase. In addition, they also believed that the adsorption of nano-particles on the surface of small pore throats in porous media would lead to a decrease in the porosity and absolute permeability of porous media. In addition, the wettability of the same type of nanoparticles is different under the action of different dispersants,<sup>13</sup> and the changes in wettability of different nano-particles in the rock formation are also different.<sup>14</sup> Layer adsorption and wettability are affected by factors such as nanoparticle size and concentration.<sup>15–17</sup> In general, irreversible adsorption on nano-particle minerals is the core of changing wettability, while the interaction of electrostatic repulsion, non-electrostatic adhesion, and pore structure drives the change of wettability.<sup>18</sup> (2) Inhibition of the hydration expansion of clay mineral particles. Some scholars believe that nano-particles can form a hydrophobic adsorption layer on the pore surface, which effectively reduces the contact probability between clay particles and fluid in the pore throat and avoids hydration swelling.<sup>19</sup> Experimental studies have shown that clay minerals that have not been treated with nano-particles will hydrate and swell to block the pore throats after being soaked in water injection. Clay particles need to be prevented from hydration and swelling.<sup>20,21</sup> (3) Hydrophobic slip effect. Qinfeng and others summarized the drag reduction mechanism of hydrophobic nano-particles according to the related reports that the nano-lattice can greatly increase the slip effect of the fluid: the adsorption capacity of the nano-particles is stronger than that of the water layer, and the formed hydrophobic structure layer produces a fluid slip mechanism.<sup>4</sup> The principle of hydrophobic nano-particles attached to the pore wall to affect the flow resistance needs to be explored continuously and demonstrated through experiments that the nano-slip effect can be generated in micropores.<sup>5</sup>

According to the mechanism of nano-depressurization and injection enhancement, some scholars have also proposed a characterization model. According to the slip effect, Qinfeng et al.<sup>4,5</sup> used the Lattice Boltzmann method to calculate the theoretical fluid slip distance caused by the slip effect. Compared with the experimental results, the simulated results were found to be in good agreement, which verified the reliability of the model. The results preliminarily demonstrated

the basic principle of drag reduction and injection enhancement of nano-particles; Gu et al.<sup>22,23</sup> considered multiple influencing factors of nano-particle adsorption and established a targeted and corrected slip mathematical model. Through this model, the seeming contradiction between the reduction of the pore size of the adsorbed particles and the increase of the injection is explained, which shows that the hydrophobic effect generated by the adsorption of the nano-particles increases the flow rate, and the increased water injection volume is much greater than the total volume of the nano-particles, thus theoretically supporting the mechanism of nano-adsorption resistance reduction.

Based on the research on the mechanism of nano-depressurization and injection increase, this paper discusses the influence of nano-solution on rock wettability through laboratory experiments and analyzes the influence of nano-solution on the organic scale and inorganic scale plug. However, compared with the good results of the pilot experiment in the field, there is still a blank in the optimization of the injection parameters and the evaluation method of the application effect of the bio-nano-additive solution. In this paper, the injection parameters of the bio-nano-injection fluid were optimized, and the effect of the field application of the bio-nano-injection solution was evaluated, which provides a basis for the further popularization and application of the technology and also provides a reference for parameter optimization and application effect evaluation of similar technologies.

## 2. METHODS

**2.1. Experimental Methods.** *2.1.1. Materials and Reagents.* Materials use in this study were nano-solution liquid, ultrapure water, artificial core, calcite, CaCO<sub>3</sub>, asphalt heavy oil, quartz sand, liquid wax, diesel oil, crude oil, kerosene, Sudan III, and core experimental materials; a total of 30 sets of core experiments were performed in this study, and the core statistical data are shown in Table 1:

*2.1.2. Laboratory Instruments and Equipment.* Experimental instruments and equipment are shown in Table 2, and the pictures of the experimental equipment are shown in Figure 1. An ultrapure water production system was used to configure the nano-solution, an optical contact angle meter was

**Table 2. Experimental Instruments and Equipment**

name	type	manufacturer
constant flow pump	HLB-1040	Dongtai Yanshan Instrument Factory
Youpu ultrapure water manufacturing system	UPH-T10T	Sichuan Youpu Ultrapure Technology Co., Ltd.
electronic balance	JM-B 20002	Zhuji Chaoze Weighing Apparatus Co., Ltd.
ultrasonic stirrer	SYU-30-900	Zhengzhou Shengyuan Instrument Co., Ltd.
optical contact angle meter	DSA100HP	Klūth Scientific Instruments Ltd.
electron microscope	FEG Quanta250	Beijing Yicheng Hengda Technology Co., Ltd

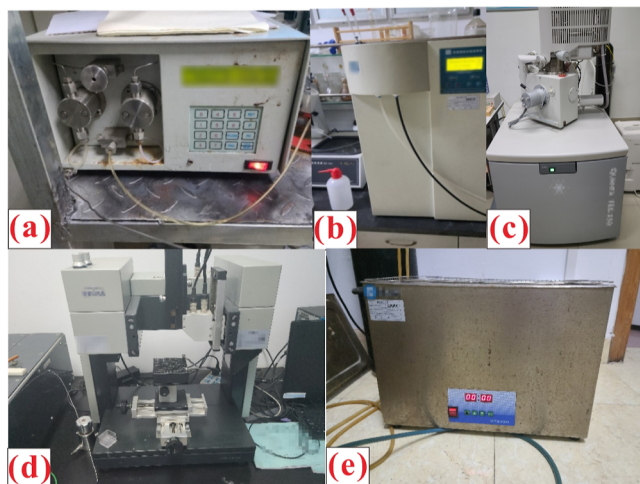


**Figure 1.** Pictures of experimental instrument [(a) constant flow pump; (b) ultrapure water manufacturing system; (c) electron microscope; (d) optical contact angle meter; and (e) ultrasonic stirrer].

used to measure the wetting angle, and an electron microscope was used to observe the effect of the nano-solution on the inorganic scale in the pores.

**2.1.3. Preparation of Samples.** Preparation of nano-solution: to 100 mL of stock nano-solution, purified water was added to make 1 L, the solution was put in an ultrasonic stirrer and stirred evenly to obtain the nano-solution. The purpose of this step was to obtain an evenly dispersed diluted nano-solution.

**2.1.4. Experimental Scheme.** There are three kinds of experiments in the bio-nano-pressure reduction and injection increase research: wettability measurement, plugging removal effect measurement, and reservoir permeability improvement effect measurement.

**2.1.4.1. Wettability Analysis Design.** The experimental steps are as follows:

- (1) Prepared rock slices are put into a beaker, the nano-solution is poured, and a vacuum pump is used to evacuate, so that the nano-solution can enter the pores of the rock;
- (2) Rock slices are put into the beaker, pure water is poured, and a vacuum pump is used to evacuate, so that the pure water enters the rock pores, as a control group;
- (3) The rock slices are dried, Sudan III is added to the kerosene, and the kerosene is dyed red;
- (4) Dyed kerosene is added into a container, the slices are added, and it is placed on the stage until no bubbles emerge;
- (5) A needle is used to draw pure water and injected on to the rock surface, and an appropriate method is selected from tangent1, tangent2, and Laplace–Young to measure the wetting angle.
- (6) The adsorbed rock sample slices are rinsed with water for 30 min, dried at a high temperature of 55 °C, and core slices are scanned with an electron microscope before and after treatment.

**2.1.4.2. Analysis Design of Inorganic Scale Plug Removal.** The experimental steps are as follows:

- (1) Determination of corrosion rate

Minerals are rinsed repeatedly with clean water, allowed to settle, the upper turbid liquid is poured out, and minerals are rinsed again. The determination of the dissolution rate of the cuttings by the pretreatment liquid and the main liquid is carried out following the China Petroleum and Natural Gas Industry Standard SY/T 5886-93 “Sandstone Retarding Acid Performance Evaluation Method”.

## (2) Scanning electron microscopy test

A scanning electron microscope is used to observe the morphology and particle size of the samples before and after modification. The surface of the samples needs to be sprayed with gold before testing.

**2.1.4.3. Analysis Design of Improving Reservoir Permeability.** The experimental steps are as follows:

- (1) Artificial cores with different permeability are selected, basic parameters such as porosity, length, diameter, etc., are measured, the core is placed into the core holder, inlet and outlet are tightened, and the confining pressure is adjusted to 2–4 MPa. The confining pressure is always greater than the inlet pressure by at least 2 MPa;
- (2) A constant current pump is used to change the flow rate to inject the nano-solution;
- (3) An electronic balance is placed at the outlet pipeline of the core holder, the fluid flowing out of the beaker is collected at the outlet, and the values of the electronic balance and the inlet pressure are recorded every 1 min;
- (4) Flow rate is calculated by calculating the difference between every two numbers, and permeability is calculated according to Darcy’s law, [formula 1](#)

$$K_{we} = \frac{q_w \mu_w L}{A(p_1 - p_2)} \times 100 \quad (1)$$

In the formula,  $K_{we}$ —effective permeability of the water phase, mD;  $q_w$ —the value of water flow, mL/s;  $\mu_w$ —the value of the viscosity of water at the measured temperature, mPa·s;  $L$ —the value of the core length, cm;  $A$ —the value of the cross-sectional area of the core, cm<sup>2</sup>;  $p_1$ —the value of the core inlet pressure, MPa; and  $p_2$ —the value of the core outlet pressure, MPa.

**2.2. Parameter Optimization Method of Bio-Nano-depressurization and Injection Enhancement Technology.** Well A1 in Bohai Oilfield is a water injection well, forming well group A1 with six oil-producing wells around it. During the injection process of Well A1, the injection pressure quickly rose to about 12 MPa in the short term, and the water injection volume gradually decreased from 110 to 75 m<sup>3</sup>/d. In the first half of 2018, the injection pressure rose to 14.5 MPa, and the daily injection volume rose to 100 m<sup>3</sup>/d. After the acidification measures were taken in the second half of 2018, the daily injection volume rose to 200 m<sup>3</sup>/d, but the water injection decreased rapidly. Before the application of the biological nanodepressurization and injection-increasing technology, the water injection pressure was as high as 18 MPa to complete the injection of 120 m<sup>3</sup>/d.

In the actual field application process, the concentration of biological nano-augmentation solution also has a great influence on the improvement effect. In order to optimize the injection parameters of the biological nano-injection fluid, a conceptual model is established by using a numerical simulation software to optimize the design of the A1 well group in Bohai Oilfield. The conceptual model established and

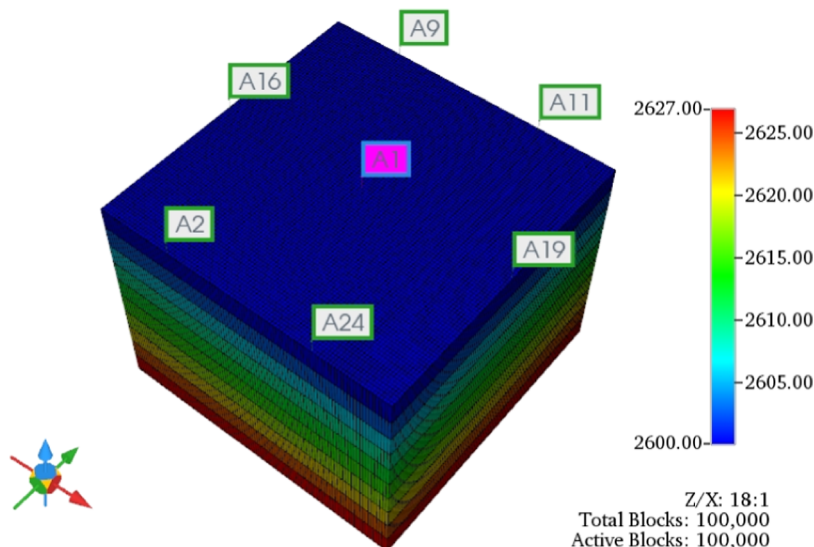


Figure 2. Schematic diagram of conceptual model.

the relative permeability used are shown in Figures 2 and 3. Then, the injection volume, injection concentration, and

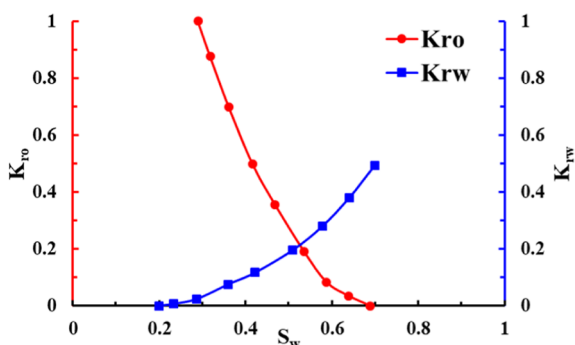


Figure 3. Relative permeability curve.

injection rate were optimized by the control variable method. The parameter optimization results will be discussed later in Section 3.2.

**2.3. Effect Evaluation Methods of Biological Nano-Depressurization and Injection Enhancement Technology.** In order to evaluate the application effect of the biological nano-injection-increasing solution, referring to the definition of residual resistance coefficient,<sup>24,25</sup> the injection-increasing capacity coefficient of the nano-solution is defined as

$$\alpha = \frac{\ln(r_e/r_w) + S_0}{\frac{K_0}{K_{\text{nano}}} \left( \ln \frac{r_f}{r_w} + S_{\text{nano}} \right) + \ln \frac{r_e}{r_f}} \quad (2)$$

where  $r_e$  is the control radius of the injection well, in meters;  $r_w$  is the bottom radius, in meters;  $S_0$  is the skin factor before the biological nano-depressurization and injection enhancement measures;  $K_0$  is the permeability before the biological nano-depressurization and injection enhancement measures, in millidarcy;  $r_f$  is the treatment radius of the biological nano-augmentation solution, in meters;  $S_{\text{nano}}$  is the skin factor after biological nano-depressurization and injection enhancement measures; and  $K_{\text{nano}}$  is the permeability after biological nano-

depressurization and injection enhancement measures, in millidarcy.

**2.3.1. Well Test Interpretation Method.** After the application of the biological nano-depressurization and injection-increasing technology, the permeability and porosity will change in the near wellbore zone, as shown in Figure 4.

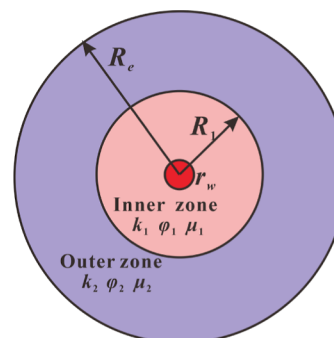


Figure 4. Schematic diagram of the influence of nano-particles on reservoir stratum.

Therefore, the well test model of biological nano-depressurization and injection enhancement is established as follows

inner zone seepage equation:

$$\frac{1}{r} \frac{\partial}{\partial r} \left( r \frac{\partial p_1}{\partial r} \right) = \left( \frac{\varphi \mu c_t}{k} \right)_1 \frac{\partial p_1}{\partial t} \quad (3)$$

outer zone seepage equation:

$$\frac{1}{r} \frac{\partial}{\partial r} \left( r \frac{\partial p_2}{\partial r} \right) = \left( \frac{\varphi \mu c_t}{k} \right)_2 \frac{\partial p_2}{\partial t} \quad (4)$$

Its boundary conditions are

well storage effect:

$$\left( r \frac{\partial p_1}{\partial r} \right)_{r=r_w} = \frac{\mu_1 B_1}{172.8 \pi k_1 h} \left( q + \frac{24C}{B_1} \frac{dp_{wf}}{dt} \right) \quad (5)$$

$$\text{skin effect: } p_{wf} = p_1|_{r=r_w} - S \left( r \frac{\partial p_1}{\partial r} \right)_{r=r_w} \quad (6)$$

$$\text{closed boundary: } \frac{\partial p_2}{\partial r}(r = R_e, t) = 0 \quad (7)$$

continuous interface pressure:

$$p_1(r = R_f, t) = p_2(r = R_f, t) \quad (8)$$

continuous interface velocity:

$$\left( \frac{k}{\mu} \right)_1 \frac{\partial p_1}{\partial r}(r = R_f, t) = \left( \frac{k}{\mu} \right)_2 \frac{\partial p_2}{\partial r}(r = R_f, t) \quad (9)$$

$$\text{initial condition: } p_1(r, t = 0) = p_2(r, t = 0) = p_i \quad (10)$$

It can be solved after Laplace transformation and Stehfest numerical inversion<sup>26</sup> and making the above eqs 3–10 dimensionless, the dimensionless pressure solution of the Laplace space can be finally obtained

$$\bar{p}_{1D} = A_1 I_0(r_D \sqrt{z}) + A_2 K_0(r_D \sqrt{z}) \quad (11)$$

$$\bar{p}_{2D} = A_3 J_0(r_D \sqrt{\lambda_{12} z / \omega_{12}}) + A_4 K_0(r_D \sqrt{\lambda_{12} z / \omega_{12}}) \quad (12)$$

$$\bar{p}_{wFD} = A_1 [I_0(r_{wD} \sqrt{z}) - S \sqrt{z} I_1(r_{wD} \sqrt{z})] + A_2 [K_0(r_{wD} \sqrt{z}) + S \sqrt{z} K_1(r_{wD} \sqrt{z})] \quad (13)$$

In the above equations,  $z$  is the Laplace variable;  $\lambda_{12}$  is the ratio of the pressure conductivity coefficients of the inner zone and outer zone,  $\lambda_{12} = (k/\mu)_1 / (k/\mu)_2$ ;  $\bar{p}_{1D}$ ,  $\bar{p}_{2D}$ ,  $\bar{p}_{wFD}$  are dimensionless pressure values in inner zone, outer zone, and bottom hole Laplacian space, respectively;  $I_0$  and  $K_0$  are the first and second modified Bessel functions of zero order, respectively;  $I_1$  and  $K_1$  are the first and second modified Bessel functions of first order, respectively; and  $A_1$ ,  $A_2$ ,  $A_3$ , and  $A_4$  are the coefficients, which can be determined by initial and boundary conditions. For the derivation process of the concrete, our previous work can be referred.<sup>27</sup>

The permeability, skin factor, and other parameters can be obtained by taking the well test data into it.

**2.3.2. Water Absorption Index Method.** The water absorption index of the water injection well after the treatment of biological nano-augmentation fluid meets

$$\frac{q_{inj}(t)}{\Delta p(t)} = \frac{1}{b} e^{-m/bt} \quad (14)$$

where

$$m = 1.53 \frac{B}{\phi h \mu C_A} \quad (15)$$

$$b = 20.62 \frac{B \mu}{K h} \ln \left( \frac{4A}{e \gamma C_A r_w'^2} \right) \quad (16)$$

where  $A$  is the control area of the injection well,  $A = \pi r_e^2$ , in square meters;  $r_e$  is the control radius, in meters;  $\gamma$  is Euler's variable, the value is 0.577216; and  $C_A$  is the reservoir shape factor.

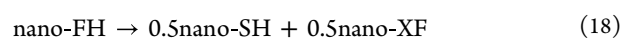
Transforming eq 14 into a linear form gives

$$\ln \left( \frac{\Delta p(t)}{q(t)} \right) = \frac{m}{b} t + \ln b \quad (17)$$

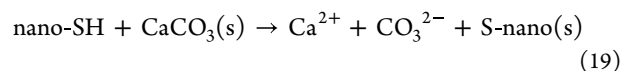
After fitting the relationship between the water absorption index and time, the permeability can be obtained by substituting it into eq 16.

**2.3.3. Numerical Simulation Method.** Before field application, the biological nano-injection-increasing fluid will be moderately acidified to make it easier to inject into the formation. Therefore, there are two main mechanisms of the biological nano-depressurization and injection enhancement technology: (1) dissolving inorganic scale and (2) nanometer materials are adsorbed to form a nanomembrane, reducing seepage resistance.

Assuming that the number of injected nano-particles in the two mechanisms is equal, the injected nanocomposite components will react to generate nano-particle components corresponding to the two mechanisms



The first action mechanism of half of the nano-particles is to dissolve inorganic scale. The chemical reaction is as follows



Inorganic scale  $\text{CaCO}_3$  is dissolved and then transformed into S-nano with a smaller density, resulting in a decrease in porosity. The Carmen Kozeny formula option in the variable permeability option can simulate the improvement of water phase permeability.<sup>28,29</sup>

$$\left( \frac{K}{K_0} \right) = \left( \frac{\phi}{\phi_0} \right)^n \left( \frac{1 - \phi_0}{1 - \phi} \right)^2 \quad (20)$$

where  $K$  is the absolute permeability after biological nano-measure,  $\phi$  is the porosity after the biological nano-measure,  $K_0$  is the absolute permeability before the biological nano-measure, and  $\phi_0$  is the porosity before biological nano-measure.

The numerical simulation model is established as follows

$$\begin{aligned} \nabla \cdot \left[ c_{np} \frac{KK_{rw}}{\mu_w B_w} \nabla \left( \frac{\partial P_w}{\partial x} - \gamma_{np} \frac{\partial D}{\partial x} \right) \right] + \nabla \cdot [d_p \phi S_w \nabla c_{np}] + q_w c_{np} \\ = \frac{\partial(\phi S_w c_{np})}{\partial t} + \frac{\partial[F_{np} \rho_{np} (1 - \phi) \hat{c}_{np}]}{\partial t} + \frac{\partial c_{np}}{\partial t} \end{aligned} \quad (21)$$

where  $c_{np}$  is the concentration of the biological nano-solution,  $K_{rw}$  is the relative permeability of the aqueous phase,  $\mu_w$  is the viscosity of the aqueous phase,  $B_w$  is the volume coefficient of the aqueous phase,  $S_w$  is the water saturation,  $x$  is the distance from the bottom hole,  $P$  is the formation pressure,  $d_{np}$  is the diffusion coefficient of the nano-particles;  $F_{np}$  is the percentage of pore surface in contact with water;  $\gamma_{np}$  is the specific gravity of increased injection nano-solution;  $D$  is the grid size; and  $\rho$  is the density of nano-particles.

In the numerical simulation, the relative permeability data used is the curve data in Figure 3, and the geological model is shown in Figure 5.

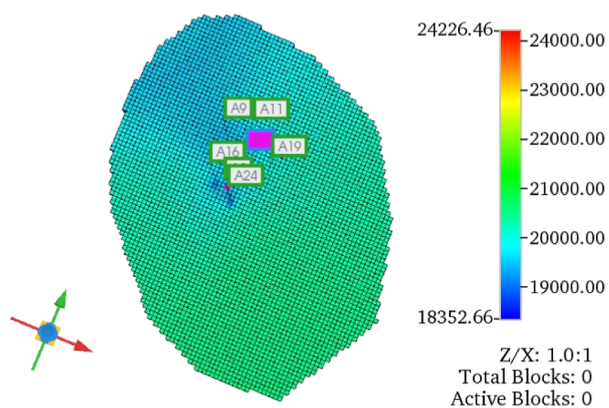


Figure 5. Schematic diagram of the geological model.

After simulating the actual area with the numerical simulation software, the permeability, skin factor, and other parameters can be obtained.

In this section, aiming at the evaluation methods of the effect of biological nano-pressure reduction and injection technology, methods are proposed from three aspects: well testing, water absorption index, and numerical simulation. These methods are then applied to the actual field to verify the accuracy.

### 3. RESULTS AND DISCUSSION

**3.1. Experimental Results and Discussion.** *3.1.1. Effect of Biological Nano-solution on Rock Wettability.* It can be seen from Figure 6 that the wetting angle of the core after treatment with the nano-solution increases significantly. The average initial wetting angle of the low permeability core is  $112.17^\circ$ , which rises to  $136.5^\circ$  after being treated with nano-solution; the average initial wetting angle of the medium-permeability core is  $113.49^\circ$ , which rises to  $138.51^\circ$  after being treated with nano-solution. Both the core wetting angles are increased by nearly  $20^\circ$ , which greatly increases the hydrophobicity of the cores.

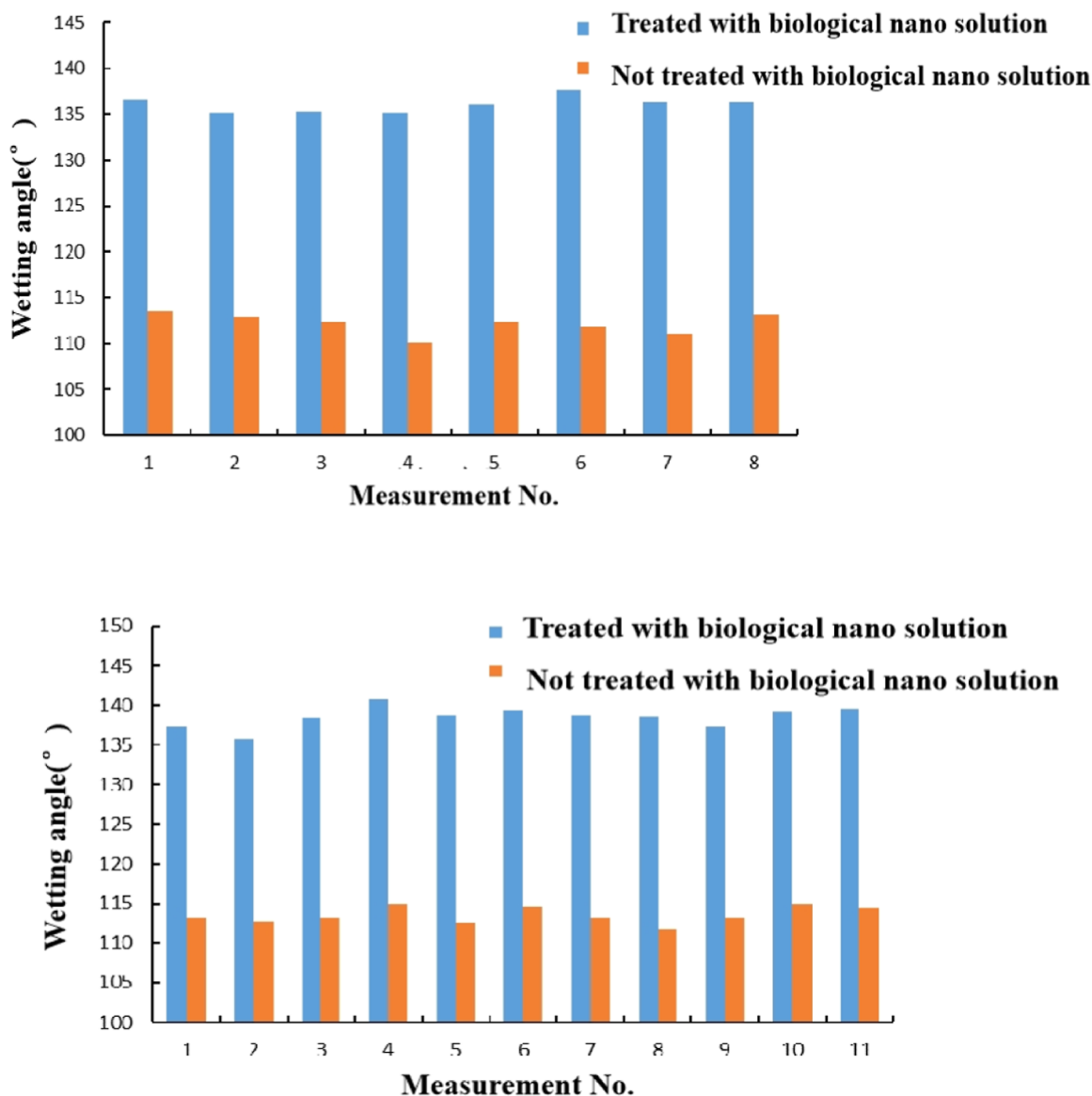
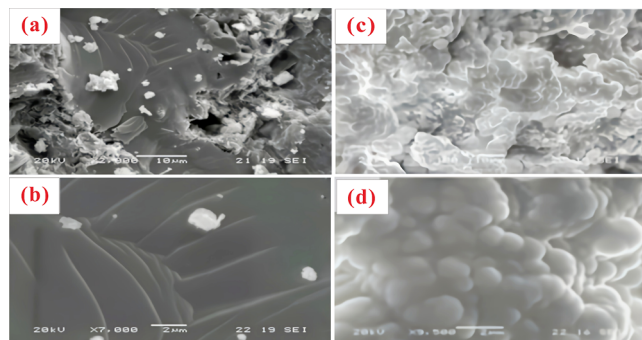


Figure 6. Influence of injected PV number on core permeability. (a) Effect of nano-solution on the wetting angle of the low-permeability core. (b) Effect of nano-solution on the wetting angle of the medium-permeability core.

It can be seen from the scanning electron microscopy (SEM) pictures of rock slices before and after adsorption, as shown in Figure 7, that there is a certain amount of highly



**Figure 7.** SEM image of rock slice [(a,b) blank, (c,d) adsorbed bio-nano].

hydrophilic minerals such as quartz and clay in the rock; so the wettability is highly hydrophilic. This kind of rock has a small surface energy. When water drops on it, it is easy to be adsorbed by minerals and clay, which will be wetted quickly, and it is difficult to form a contact angle; after bio-nano-solution treatment, the surface of clay minerals in the rock is covered by hydrophobic nano-particles. Because the surface of the covered nano-particles is hydrophobic, its surface energy increases. When water drops on it, it becomes spherical under the action of energy minimization and gravity, and the wettability of the rock surface changes to hydrophobicity. When the fluid passes through the pores, its flow resistance will be reduced, and the flow velocity and discharge will be increased to achieve the effect of reducing pressure and increasing injection.

**3.1.2. Effect of Biological Nano-solution on an Inorganic Scale.** **3.1.2.1. Inorganic Scale Dissolution in Nano-solution.** Table 3 and Figure 8 show that the corrosion rate of the 1:2 and 1:3 bio-nano-solution systems has reached about 43%, showing a high corrosion effect and greatly improving the corrosion rate. With the decrease in concentration, the corrosion rate decreases. The main reason may be that the concentration of active components in the system decreases. During the concentration reduction, the system can still maintain a certain corrosion rate of 18%. It has a good corrosion effect.

From the above evaluation, it can be seen that the nano-solution has a good corrosion effect on minerals. During the corrosion process, the turbidity in the nano-solution is not high, and there are few secondary reservoir damage substances, which is conducive to the protection of oil and gas reservoirs. Meanwhile, the nano-solution dissolution of minerals can also effectively increase the pore throat radius to increase the injection volume. The solution has a good effect of stabilizing metal ions, which can achieve scale inhibition, scale prevention,

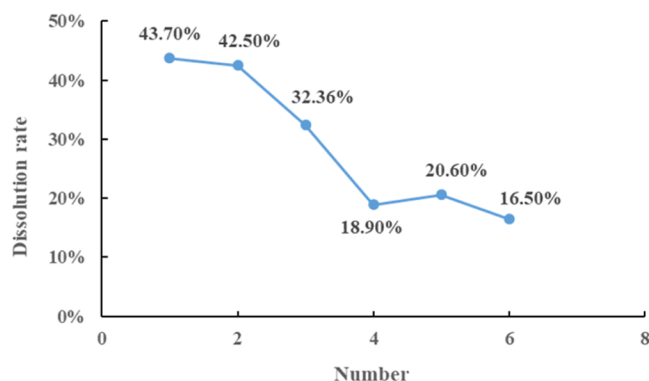


**Figure 8.** Results of the determination of the corrosion rate.

and reduce the secondary damage of sandstone acidification. There are also many coordination atoms in the molecule, which can form stable chelates.

**3.1.2.2. Mineral Dissolution SEM.** Through SEM, the microscopic observation shows that the mineral surface morphology changes after the action of plugging removal fluid, as shown in Figures 9 and 10.

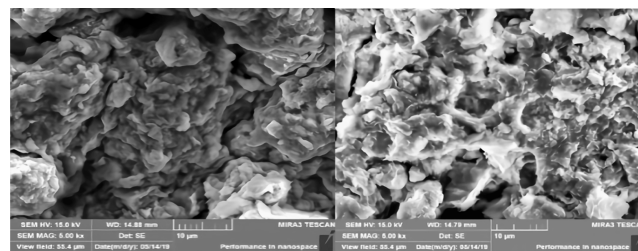


**Figure 9.** SEM images of minerals (montmorillonite) before and after dissolution.



**Figure 10.** SEM images before and after dissolution of cuttings.

As can be seen from the SEM picture (the scale is 10  $\mu\text{m}$ ) in Figure 9, before the plug removal and corrosion process, the mineral mixture is closely bound and the pores/micropores between minerals are few. After acidification, the mineral edges are clear, the pore structure between minerals increases, and a large number of micropores appear.

As can be seen from the SEM picture (scale is 1  $\mu\text{m}$ ) in Figure 10, before the dissolution process, the surface and edges

**Table 3.** Table of Results of Determination of Corrosion Rate

number	1	2	3	4	5	6	unit
reaction time	1:2	1:3	1:4	1:5	1:6	1:7	g
mineral mixture	5						g
Bake to Constant Weight: 105 °C 24 h							
dissolution rate	43.7%	42.5%	32.36%	18.9%	20.6%	16.5%	

of montmorillonite mineral/cuttings are smooth, and the surface is covered with a layer of material. After the dissolution, the mineral surface is rough and uneven, with obvious dissolution holes and pits, and the particle surface is brittle. SEM results show that the nano-solution can effectively dissolve minerals, expand the pores, cracks, and holes in contact with them, and play a good role in removing inorganic scale.

In this section, the effects of biological nano-solution on rock wettability and inorganic scale are studied experimentally. The experimental results show that the bio-nano-injection-increasing solution can obviously change the rock wettability into hydrophobicity, the flow resistance decreases, and the overall flow velocity and discharge increase significantly. Nano-solution can also remove inorganic scale and organic scale, so as to enlarge pore space and increase injection.

**3.1.3. Effect of the Bio-Nano-fluid on Permeability.** The biological nano-injection fluid is mainly composed of biological nano-dispersion fluid, hydrophobic nano-polysilicon, and dispersant additives. Its main depressurization and augmentation injection mechanism is to form a hydrophobic film on the pore wall, so that water phase slip can be formed in the process of injection water flow, so as to reduce the seepage resistance and greatly reduce the injection pressure. This can be characterized using permeability instead.

**3.1.3.1. Effect of Injected Volume of Bio-Nano-Augmentation Fluid on Permeability.** A core with an initial permeability of 18 mD was selected for the displacement test, and the experimental results are shown in Figure 11.

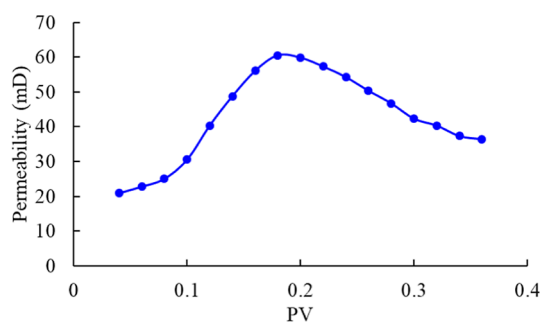


Figure 11. Influence of injection volume on permeability.

It can be seen from Figure 11 that the injection of biological nano-augmentation fluid can significantly improve the core permeability, and with the increase of injected PV (pore volume multiple), it shows a trend of first increasing and then decreasing, that is, there is an optimal injection volume.

**3.1.3.2. Effect of Injection Rate of Bio-Nano-Augmentation Fluid on Permeability.** A core with an initial permeability of 51 mD was selected for displacement experiments at different flow rates. The experimental results are shown in Figure 12.

It can be seen from Figure 12 that different flow rates of the bio-nano-injection solution have different effects on the improvement effect, and the increase of injection rates leads to the improvement effect becoming better first and then worse.

In this section, the effects of injection volume and injection rate of bio-nano-injection-increasing solution on reservoir permeability are studied through core displacement experiments. The results show that there is an optimal value of

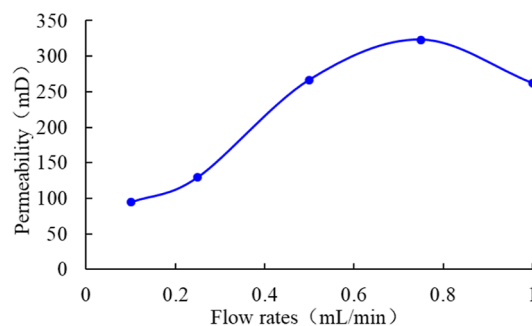


Figure 12. Influence of injection rate on permeability.

injection volume and injection rate, and the injection effect will decrease if the value is exceeded.

### 3.2. Parameter Optimization Results and Discussion.

**3.2.1. Optimization of the Injection Volume.** The injection concentration was set as 1200 ppm, the injection rate was 120 m<sup>3</sup>/d, and the PV numbers of biological nano-augmentation solution were 0.000234, 0.000268, 0.000292, 0.000326, and 0.000358. The application effects of biological nano-augmentation solution with different volumes are shown in Figure 13.

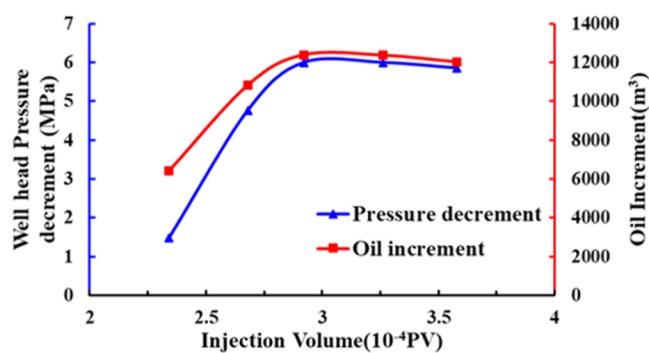


Figure 13. Influence of injection volume on application consequent.

It can be seen from Figure 13 that the larger the injection volume, the better the application effect, but the application effect will slowly deteriorate after exceeding a certain extent; when the injection volume is 0.000292PV, the wellhead pressure drops and oil increase can achieve good application effect.

**3.2.2. Optimization of the Injection Concentration.** The injection PV was set to 0.000292, the injection rate to 120 m<sup>3</sup>/d, and the injection concentrations of biological nano-solution to 600, 900, 1200, 1800, and 2400 ppm. The application effects of biological nano-augmentation solution with different concentrations are shown in Figure 14.

It can be seen from Figure 14 that the higher the injection concentration is, the better the application effect is. However, after exceeding a certain degree, the application effect will not get better, or even get worse slowly; when the injection concentration is 1200 ppm, the wellhead pressure drop and oil increase can achieve a good application effect.

**3.2.3. Optimization of the Injection Rate.** The injection PV was set as 0.000292, the injection concentration as 1200 ppm, and the injection rates of biological nano-augmentation fluid as 110, 115, 120, 125, 130, and 135 m<sup>3</sup>/d. The application effects of biological nano-augmentation fluid with different injection rates are shown in Figure 15.

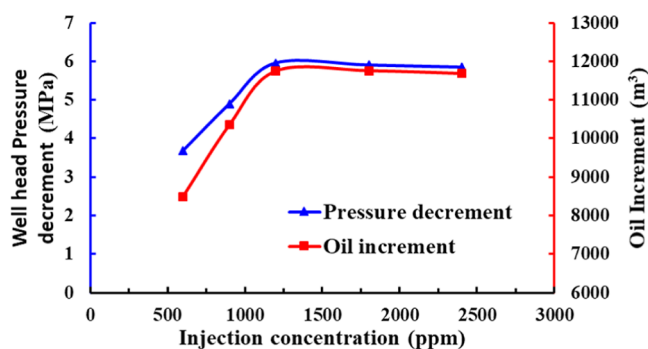


Figure 14. Influence of injection concentration on application consequent.

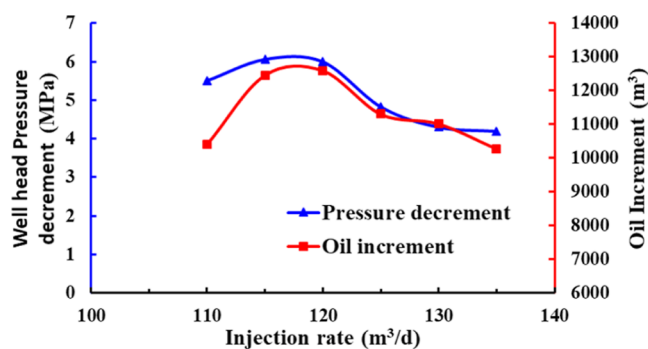


Figure 15. Influence of injection rate on application consequent.

It can be seen from Figure 15 that with the increase of the injection rate, the wellhead pressure drop value and the oil increase amount first increase and then decrease, that is, there is an optimal value ( $120 \text{ m}^3/\text{d}$ ).

In this section, numerical simulation was used to optimize the injection volume, injection concentration, and injection rate of the bio-nano-depressurization and injection enhancement technology. Taking well group A1 as an example, the numerical simulation results show that the recommended injection rate is  $0.000292\text{PV}$ , the injection concentration is  $1200 \text{ ppm}$ , and the injection rate is  $120 \text{ m}^3/\text{d}$ . If it exceeds the recommended value, the results will not be optimal.

**3.3. Field Application Results and Discussion.** In July 2019, the biological nano-plugging removal and injection-

increasing measures were taken for well group A1 in Bohai Oilfield. After the measures, the injection pressure dropped significantly at the beginning, to about  $7\text{--}9 \text{ MPa}$ , which was  $10 \text{ MPa}$  lower than before, and the pressure reduction range reached  $56\%$ , showing an obvious pressure drop effect. One year after the measures, the injection pressure gradually increased to  $10\text{--}12 \text{ MPa}$ , still maintaining a certain pressure drop effect. The corresponding daily injection volume rose to  $150\text{--}200 \text{ m}^3/\text{d}$  at the beginning,  $55 \text{ m}^3/\text{d}$  more than that before the measure, and the injection increase reached  $46\%$ . The injection rate of water injection wells significantly increased. One year after the measure was implemented, the injection volume decreased to  $130\text{--}150 \text{ m}^3/\text{d}$ , and the effect of pressure reduction and injection increase was still good.

In order to quantitatively evaluate the application effect of biological nano-injection technology, A1 well was selected to use the above three methods to evaluate the effect of biological nano-depressurization and injection technology.

**3.3.1. Analysis by the Well Test Interpretation Method.** The well test fitting analysis results from Figure 16 show that the near well permeability of Well A1 changed from  $280.60$  to  $670 \text{ mD}$ , and the skin factor changed from  $4.66$  to  $0.668$  after the treatment of biological nano-injection fluid. Bio-nano-depressurization and injection-increasing technology can effectively improve the formation permeability around injection wells.

**3.3.2. Analysis by the Water Absorption Index Method.** It can be seen from the Figure 17 that  $b = -2.941$ . After the calculation of eq 16, it is found that the near well permeability of Well A1 changes from  $280.60$  to  $797.59 \text{ mD}$  after the treatment of biological nano-injection fluid. Bio-nano-depressurization and injection-increasing technology can effectively improve the formation permeability around injection wells.

**3.3.3. Analysis by the Numerical Simulation Method.** Using the numerical simulation method, the near well permeability changes from  $280.60$  to  $736.4 \text{ mD}$ .

The permeability and injection-increasing capacity coefficient calculated by several methods are shown in Table 4. It can be seen from Table 4 that the three methods can be used to evaluate the performance of the biological nano-depressurization and injection-increasing composite system, and the methods have certain accuracy.

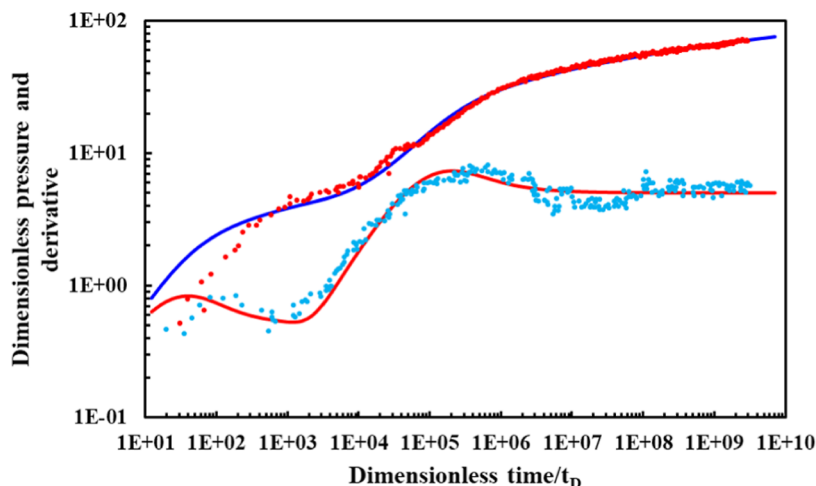


Figure 16. Fitting diagram of well testing.

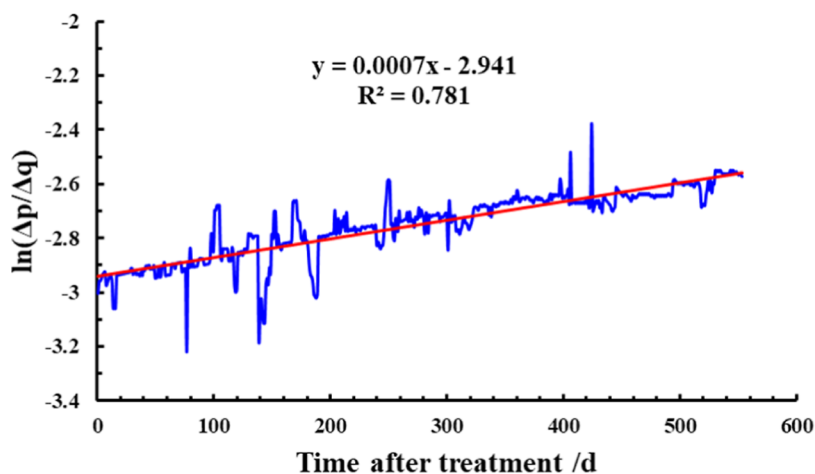


Figure 17. Fitting diagram of apparent water injectivity index.

Table 4. Permeability and Injection Enhancement Coefficient of Well A1 in Bohai Oilfield before and after Bio-Nano-Depressurization and Injection Enhancement Technology

parameter	permeability before measures	well test interpretation method	water absorption index method	numerical simulation method
permeability/mD	280.60	670	803.87	736.40
injection-increasing capacity coefficient		2.285	2.452	2.376

#### 4. CONCLUSIONS

The bio-nano-injection-increasing solution is composed of dispersant aids, biosurfactants, and hydrophobic nano-poly-silicon particles. It has the dual advantages of high-efficiency depressurization and environmental friendliness and has shown good results in field experiments. The following conclusions are drawn from the optimization of the injection parameters of the biological nano-augmentation solution and the application effect.

- (1) Biological nano-technology is a long-term injection-increasing technology that integrates multiple functions such as nano-scale inhibition, wetting reversal, hydration expansion inhibition, particle migration prevention, and high-efficiency pressure reduction.
- (2) The influence of nano-solution on rock wettability is discussed: the core wettability becomes hydrophobic after being treated with nano-solution, which reduces the flow resistance, significantly increases the overall flow velocity and flow, and produces a significant depressurization effect.
- (3) The nano-solution is helpful to disperse the organic scale after stripping and avoid the secondary precipitation blockage of the organic scale after stripping; nano-solution can effectively dissolve minerals, expand the pores, cracks, and holes in contact with them, and play a good role in removing inorganic scale.
- (4) The biological nano-injection fluid can effectively improve the reservoir permeability and reduce the injection pressure of injection wells.
- (5) There is an optimal injection parameter for the biological nano-augmentation solution. If the injection parameters exceed this value, the improvement effect will not increase significantly or even become worse. The recommended injection volume of well group A1 is 0.000292PV, the injection concentration is 1200 ppm, and the injection rate is 120 m<sup>3</sup>/d.

- (6) The evaluation method for the application effect of biological nano-depressurization and injection-increasing technology is proposed from three directions of well testing, water absorption index, and numerical simulation. The injection-increasing capacity coefficients calculated by the three methods are 2.285, 2.452, and 2.376, respectively, with little difference in calculation results and high accuracy.

#### ■ AUTHOR INFORMATION

##### Corresponding Authors

Xianchao Chen – College of Energy, Chengdu University of Technology, Chengdu 610059, China; [orcid.org/0000-0003-0576-5259](https://orcid.org/0000-0003-0576-5259); Email: [chenxianchao2005@126.com](mailto:chenxianchao2005@126.com)

Yuehui She – College of Petroleum Engineering, Yangtze University, Wuhan, Hubei 430100, China; Hubei Key Laboratory of Drilling and Production Engineering for Oil and Gas, Wuhan 430010, China; Email: [sheyuehui@163.com](mailto:sheyuehui@163.com)

##### Authors

Qing Feng – Oilfield Production Optimization Institution of China Offshore Oilfield Services Limited, Tianjin 300459, China

Ning Zhang – Tianjin Branch of CNOOC (China) Co., LTD, Tianjin 300459, P. R. China

Xiaonan Li – Oilfield Production Optimization Institution of China Offshore Oilfield Services Limited, Tianjin 300459, China

Jingchao Zhou – College of Energy, Chengdu University of Technology, Chengdu 610059, China

Shengsheng Li – Oilfield Production Optimization Institution of China Offshore Oilfield Services Limited, Tianjin 300459, China

Xiaorong Zhang – Guangdong NanYou Service Co., Ltd., Tianjin 300450, China

Yanni Sun – Guangdong NanYou Service Co., Ltd., Tianjin 300450, China

Complete contact information is available at:  
<https://pubs.acs.org/10.1021/acsomega.3c00882>

## Notes

The authors declare no competing financial interest.

## ACKNOWLEDGMENTS

The authors are grateful for funding from the National Natural Science Foundation of China (grant nos 51804048, 21974014).

## REFERENCES

- (1) Zhou, Y.-B.; He, Y.-F.; Zhang, W.; Zhang, J.-L.; Yang, L. Economic Limit Water Cut of Single Well in Offshore Waterflooding Oilfield. *Lithol. Reservoirs* **2019**, *31*, 130–134.
- (2) Zhang, Y.-L.; Liao, X.-W.; Hu, Y.; Li, T.-L.; Su, J.-C. Development Models for Offshore Heavy Oil Field in High Water Cut Stage. *Lithol. Reservoirs* **2018**, *30*, 120–126.
- (3) Du, H.-R.; Jiang, S.-X.; Zhao, W.-M.; Chen, J.-F.; Miao, B. Analysis on the regular of acid stimulation of low permeability sandstone reservoirs. *Pet. Drill. Tech.* **2008**, *36*, 61–63.
- (4) Qinfeng, D.; Shen, C.; Wang, Z.-H.; Gu, C.-Y.; Shi, L.-Y.; Fang, H.-P. Experimental research on drag reduction of flow in micro channels of rocks using nano-particle adsorption method. *Acta Pet. Sin.* **2009**, *30*, 125–128.
- (5) Di, Q.-F.; Li, Z.-H.; Shi, L.-Y.; Wu, F.; Gu, C.-Y.; Yu, Z.-B. Effect of hydrophobic nanoparticles SiO<sub>2</sub> on flow characteristics in microchannel. *J. Univ. Pet., China* **2009**, *33*, 109–111.
- (6) Zhai, H.; Qi, N.; Sun, X.; Zhang, X.-Y.; Fan, J.-C. Preparation and Evaluation of a New Type Step-down Augmented Injection Agent Made of SiO<sub>2</sub> Nanoparticles. *Mater. Rep.* **2019**, *33*, 975–979.
- (7) Li, Y.; Di, Q.-F.; Hua, S.; Ye, F.; Zhang, J.-L.; Wang, W.-C. Research progress in improving oil recovery by inversion of reservoir wettability with nanofluids [J]. *Chem. Ind. Eng. Prog.* **2019**, *38*, 3612–3620.
- (8) Wang, J.; Wu, Y.-H.; Deng, H.; Jin, T.-H. Effect of nano SiO<sub>2</sub>/surfactant on oil-water interfacial tension [J]. *Energy Chem. Ind.* **2018**, *39*, 7–11.
- (9) Li, X.; Feng, Q.; Gao, P.; Huang, Z.-J.; Gong, R.-X.; Chen, X.-C.; Li, J. Application Progress of Nano-SiO<sub>2</sub> in Enhanced Oil Recovery and Depressurization and Injection-augmenting. *Sci. Technol. Eng.* **2021**, *21*, 8291–8300.
- (10) Gao, P.; Feng, Q.; Chen, X.-C.; Li, S.-S.; Sun, Y.-N.; Li, J.; Zhou, J.-C.; Qian, F. Numerical simulation and field application of biological nano-technology in the low- and medium-permeability reservoirs of an offshore oilfield. *J. Pet. Explor. Prod. Technol.* **2022**, *12*, 3275–3288.
- (11) Feng, Q.; Zhou, J.-C.; Li, S.-S.; Chen, X.-C.; Sun, Y.-N.; Zhang, X.-R.; Gao, P.; Zhang, F.; She, Y.-H. Research on Characterization Technology and Field Test of Biological Nano-oil Displacement in Offshore Medium- and Low-Permeability Reservoirs. *ACS Omega* **2022**, *7*, 40132–40144.
- (12) Ju, B.-S.; Dai, S.-G.; Luan, Z.-A.; Zhu, T.-G.; Su, X.-T.; Qiu, X.-F. A study of wettability and Permeability change caused by adsorption of nanometer structured polysilicon on the surface of porous media. *SPE-Asia Pacific Oil and Gas Conference*, 2002; pp 915–926.
- (13) Maghzi, A.; Mohebbi, A.; Kharrat, R.; Ghazanfari, M. H. Pore-Scale Monitoring of Wettability Alteration by Silica Nanoparticles During Polymer Flooding to Heavy Oil in a Five-Spot Glass Micromodel. *Transp. Porous Media* **2010**, *87*, 653–664.
- (14) Roustaei, A.; Moghadasi, J.; Bagherzadeh, H.; Shahrabadi, A. An experimental investigation of polysilicon nanoparticles' recovery efficiencies through changes in interfacial tension and wettability alteration. *Society of Petroleum Engineers-SPE International Oilfield Nanotechnology Conference*, 2012; pp 200–206.
- (15) Li, S.; Torsæter, O.; Lau, H. C.; Hadia, N. J.; Stubbs, L. P. The Impact of Nanoparticles Adsorption and Transport on Wettability Alteration of Water Wet Berea Sandstone. *SPE/IATMI Asia Pacific Oil & Gas Conference and Exhibition*, 2015.
- (16) Li, S.; Dan, D.; Lau, H. C.; Hadia, N. J.; Torsæter, O.; Stubbs, L. P. Investigation of Wettability Alteration by Silica Nanoparticles Through Advanced Surface-Wetting Visualization Techniques. *SPE Annual Technical Conference and Exhibition*, 2019; pp 1–16.
- (17) Jiang, R.; Li, K.; Horne, R. A Mechanism Study of Wettability and Interfacial Tension for EOR Using Silica Nanoparticles. *SPE Annual Technical Conference and Exhibition*, 2017.
- (18) Afekare, D. Enhancing Oil Recovery Using Aqueous Dispersions of Silicon Dioxide Nanoparticles: The Search for Nanoscale Wettability Alteration Mechanism. *SPE Annual Technical Conference and Exhibition*, 2020.
- (19) Gu, C.-Y.; Di, Q.-F.; Jing, B.-H.; Wang, J.-H.; Shen, L.; Shi, W.-C. Mechanism of Hydrophobic Nano-SiO<sub>2</sub> Material in Inhibiting Clay Swelling. *Acta Pet. Sin.* **2012**, *33*, 1028–1031.
- (20) Yi, H.; Sun, H.-H.; Li, F.-X.; Li, W.-H. Decompression and Augmented Injection Theories Research of Nanometer Polesilicon in Oilfield Water Flood Development. *Nat. Sci. J. Harbin Norm. Univ.* **2005**, *21*, 66–69.
- (21) Yi, H.; Zhang, X. Experimental study of ecompression and augmented injection of polesilicon in off reservoir. *J. Mol. Sci.* **2008**, *24*, 325–328.
- (22) Gu, C.-Y.; Di, Q.-F.; Shi, L.-Y.; Wang, X.-L.; Zhang, R.-L. Model of microscopic force action of drag-reducing functional nanomaterials in petroleum reservoir pores. *Proceedings of the 9th National Conference on Hydrodynamics and the 22nd National Symposium on Hydrodynamics*, 2009.
- (23) Gu, C.-Y.; Li, G.-J.; Di, Q.-F.; Zhang, J.-L.; Qin, R.-S. A advanced slip model of adsorption layer of nano particles in homogeneous porous media. *J. Hydrodyn.* **2016**, *31*, 714–720.
- (24) Zhang, Z.-J.; Li, F.; Wei, J.; Zhou, X.; Yuan, W.-J. An Innovative Technique to Determine Underground Viscosity of Polymer. *Special Oil Gas Reservoirs* **2018**, *25*, 109–111.
- (25) Zhang, Z.-J.; Wang, H.-S.; Wei, J.; Zhou, X.; Yin, P.; Xu, H. A new method for calculating resistance coefficient in early polymer flooding. *Complex Hydrocarbon Reservoirs* **2020**, *13*, 58–61.
- (26) Tong, D.-K.; Chen, Q.-L. A note on the Stehfest method for Laplace Numerical Inversion. *Acta Pet. Sin.* **2001**, *22*, 91–92.
- (27) Feng, Q.; Gao, P.; Chen, X.-C.; Li, J.; Zhou, J.-C.; Qian, F.; Li, S.-S.; Sun, Y.-N.; Wang, Y.-Y. Development and Application of Well-Test Model after Injection Biological Nanomaterials. *Geofluids* **2022**, *2022*, 1–16.
- (28) Lijun, L.; Jun, Y.; Hai, S.; Zhaoqin, H.; Xia, Y.; Longlong, L. Compositional modeling of shale condensate gas flow with multiple transport mechanisms. *J. Petrol. Sci. Eng.* **2019**, *172*, 1186–1201.
- (29) Zheng, B.; Li, J.-H. A New Fractal Permeability Model for Porous Media Based on Kozeny-Carman Equation. *Nat. Gas Geosci.* **2015**, *26*, 193–198.